Broadband Dielectric Spectroscopy of Polymers with Hidden β Relaxation

Gustavo Dominguez-Espinosa,† Ricardo Díaz-Calleja,† and Evaristo Riande*

Departamento de Termodinámica Aplicada, ETSII, Universidad Politécnica de Valencia, Valencia, Spain, and Instituto de Ciencia y Tecnología de Polímeros (CSIC), 28006 Madrid, Spain

Received March 28, 2006; Revised Manuscript Received May 18, 2006

ABSTRACT: This work reports the relaxation behavior of amorphous polymers the spectra of which do not explicitly present the secondary β relaxation. Poly(2,4-difluorobenzyl methacrylate), a polymer with complex motions in the side groups, was chosen to carry out this study. The apparent distribution of retardation times of the polymer calculated from dielectric loss isotherms in a wide range of temperatures ($T > T_g$) presents two peaks which do not merge into a single absorption at moderate temperatures. The β absorption appearing as a shoulder of the α relaxation in global thermal stimulated depolarization current experiments is not at first sight detected in the retardation spectra. Separation of the hidden β absorption from the longest time peak in the retardation spectra was carried out by fitting the inverse of the Havriliak−Negami equation to the peak using $b = 1$ and $b < 1$ for the skewness shape parameter of the β and α relaxations, respectively. Moreover, the shortest time peak in the retardation spectra was found to be the result of two overlapping peaks, named in increasing order of time γ and γ'. Arrhenius plots for the α and β absorptions present a new scenario characterized for displaying both relaxations the same temperature dependence at temperatures not far above T_g. To investigate how small differences in the chemical structure may influence the dielectric response of polymers to perturbation fields, the results obtained for poly(2,4-difluorobenzyl methacrylate) are compared with those previously reported for poly(3-fluorobenzyl methacrylate). The differences in the responses of both polymers are interpreted in terms of molecular motions of the side groups.

Introduction

The retardation spectra of the compliance functions of high molecular weight supercooled liquids present at short times a relatively weak peak associated with localized motions followed in increasing order of time for a prominent peak arising from micro-Brownian segmental motions, named β and α absorptions, respectively. As temperature increases, both absorptions are shifted to shorter times until the high activation energy α relaxation catches the β forming the $\alpha\beta$ process.[1,2] Besides the α and β absorptions, mechanical retardation spectra of high molecular weight supercooled liquids present at long times the normal mode process associated with motions of the whole chain that govern the flow properties.[3,4] Only the dielectric retardation spectra of polar polymers with dipole components parallel to the chain contour display the normal mode process.[5] Whereas the average time associated with the α relaxation of entangled chains is nearly insensitive to chains length, the relaxation time of the normal process scales with the 3.4 and the first power of the molecular weight M, respectively, for $M > 2\ M_e$ and $M < 2\ M_e$, where M_e is the molecular weight between entanglements.[6]

The temperature dependence of both the α relaxation and the normal mode process is often found to obey the Vogel−Fulcher−Tammann−Hesse (VFTH) equation.[7] Their respective average retardation times experience an anomalous increase in the vicinity of the glass transition temperature in such a way that the α relaxation and the normal mode process become frozen at T_g, and only the β relaxation and even faster relaxations remain operative in the glassy state. For most polymers, dipoles associated with the repeating unit have not components parallel to the chain contour and as a result the normal mode process is absent in the spectra. The α relaxation (precursor of the glassy state and flow) and the β process, which for most low molecular weight supercooled liquids are detected at extremely high frequencies and/or low temperatures, are shifted to more accessible temperature/frequency windows for polymers. This fact facilitates the study of the effect of the chemical structure on both chain dynamics and development of the glassy state.

The merging of the β and α processes for poly(ethyl methacrylate) (PEM) into the combined $\alpha\beta$ process through the use of applied pressure was discovered by Williams a long time ago.[1,8] Further work showed that the merging of the α and β relaxations depends on the chemical structure.[9−24] For example, a strong β relaxation in syndiotactic poly(methyl methacrylate) (PMM) dominates the dielectric losses,[13,14] a behavior not shared by the rest of poly(*n*-alkyl methacrylate)s. Further work on poly(*n*-alkyl methacrylates) showed a strong dependence of the merging of the α and β processes on the alkyl length.[20−22] More recent studies on poly(benzyl methacrylates) have shown that substitutions of hydrogen atoms in the phenyl groups of the side chains for other atoms or groups strongly affect the relaxation behavior of these substances.[23,24] The strong interdependence of the α and β processes for some of these polymers makes difficult the separation of these two relaxations. Thus, the retardation spectrum of poly(3-fluorurobenzyl methacrylate) exhibits two well separated prominent peaks in the whole temperature range ($T > T_g$), which in principle could be attributed to the β and α absorptions. However, a close inspection of the α absorption shows that it is not a simple process but a combination of α and β relaxations so that the shortest time peak is not β, but γ.[24] Proceeding with these studies further, we report in this paper the relaxation behavior poly(2,4-fluorobenzyl methacrylate) (P24FM) to find out how the two dipoles located in the phenyl group of the latter polymer

* Corresponding author. Instituto de Ciencia y Tecnología de Polímeros (CSIC). Telephone: 34-91-5622900. Fax: 34-91-5644853. E-mail: riande@ictp.csic.es

† Universidad Politécnica de Valencia.

10.1021/ma060699e CCC: $33.50
Published on Web 06/22/2006

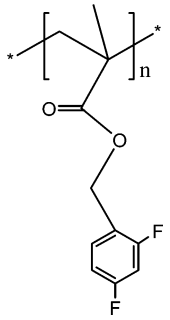

Figure 1. Scheme showing the repeating unit of poly(2,4-difluorobenzyl methacrylate)

affect its response to an electric perturbation field. The structural unit of P24FM is shown in Figure 1. As a consequence of the fact that the direction of the dipole resulting from the two dipoles located in the phenyl group of P24FM coincides with that of the $C^{ar}-F$ dipole of poly(3-fluorobenzyl methacrylate) (P3FM), we felt that it would be interesting to perform a comparative study of the dynamics of these structurally close polymers.

Molecular motions in the glassy state can also be studied at very low frequencies using thermostimulated depolarization current (TSDC) techniques in a wide temperature window. This technique, in parallel with dielectric relaxation spectroscopy (DRS), gives a deeper insight into the effect of the fine structure on secondary processes.

Experimental Part

2,4-Difluorobenzyl methacrylate was obtained at room temperature by reaction of methacryloyl chloride with 2,4-difluorophenyl methanol and further polymerized at 323 K via a free radical process. The reaction was carried out in toluene solution, under nitrogen atmosphere, using azobis(isobutyronitrile) as initiator. After 10% conversion was reached, the polymer was precipitated with methanol, dissolved in chloroform, precipitated again with methanol, and finally dried at 60 °C in a vacuum. The weight-average molecular weight of poly(2,4-fluorobenzyl methacrylate), measured by GPC, was 1.89×10^5, the heterodispersity molecular weight index lying in the vicinity of 2. The stereochemical structure of poly(benzyl methacrylate)s obtained by free radical polymerization is atactic.

The glass transition temperature, T_g, of P24FM was determined with a TA DSC-Q10 apparatus at a constant heating rate of 20 K/min, under nitrogen atmosphere. The sample was heated twice, and the middle point of the endothermic step during the second scan was taken as the glass transition temperature. The value of T_g thus obtained was 333 K.

Thermally stimulated depolarization current (TSDC) curves were obtained on polarized samples molded disks of 0.2 mm thickness and 10 mm of diameter, using a TSC/RMA TherMold 9000 apparatus. The global temperature dependence of the thermal stimulated depolarization current (TSDC) was obtained by poling the pill under an electric potential of 350 V/mm, 10 K above T_g, for 3 min, and further quenching at 113 K. Then the electric field was removed and the poled samples short-circuited for 1 min to remove free charges. Thermally stimulated depolarization curves were obtained by warming the electrode assembly at a constant heating rate of 7 K/min. From the time derivative of the polarization, the global discharge current curve as a function of temperature was obtained. Partial TSDC curves were also obtained in the glassy state, using poling windows of 5 K.

Complex dielectric permittivity measurements were performed over the frequency window 10^{-1} Hz $-$ 10^9 Hz, using a Novocontrol broad band dielectric spectrometer (Hundsangen, Germany) integrated by a SR 830 lock-in amplifier with an Alpha dielectric interface and an Agilent 4991 coaxial line reflectometer to carry out measurements in the frequency ranges $10^{-1}-10^6$ Hz and 10^6-10^9 Hz, respectively. In the latter case, the complex permittivity was determined by measuring the reflection coefficient at a particular reference plane. The temperature was controlled by nitrogen jet (QUATRO from Novocontrol) with a temperature error of $\approx$ 0.1 K during every single sweep in frequency. Isothermal measurements were carried out on molded disk shaped samples of about 0.1 mm thickness, with diameters of 20 and 10 mm for frequencies lower and higher than 10^6 Hz, respectively. Glass fiber spacers were used to ensure the stability of the sample thickness at high temperatures.

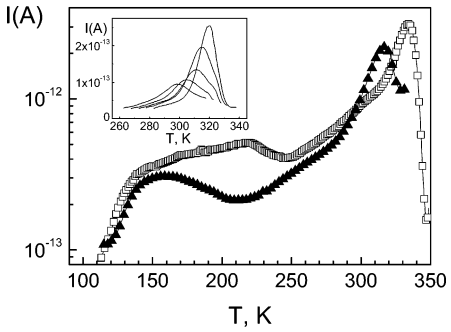

Figure 2. Global TSDC curves for P24FM (open squares) and P3FM (filled triangles). The poling temperatures for the global TSDC curves were 343 and 353 K for P3FM and P24FM, respectively. Inset: partial TSDC curves for P24FM obtained at poling temperatures from 278 to 298 K (5 K step).

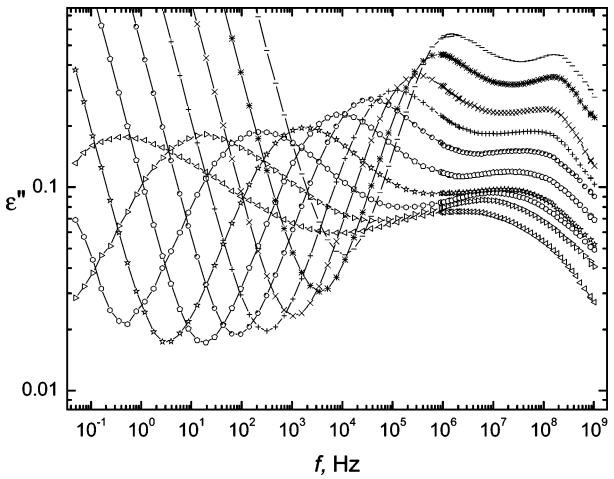

Figure 3. Experimental dielectric loss isotherms in the frequency domain for P24FM. The results cover the range of temperature 333−423 K, at 10 K steps.

Results

The temperature dependence of the global thermostimulated depolarization intensity current for P24FM is presented in Figure 2. The curve shows a broad absorption in the low-temperature region followed by a well developed process corresponding to the α relaxation. An absorption appearing as a shoulder of the α relaxation on its low-temperature side seems to correspond to the subglass β process. Partial TSDC curves were obtained in the temperature range 278−298 K using polarization windows of 5 K, and the pertinent results are shown in the inset of Figure 2. The relative high intensity of the peaks in the temperature range where the shoulder in the global TSDC curve appears reflects the presence of the secondary β absorption.

Figure 3 presents the isotherms of the dielectric loss of P24FM in the frequency domain at several temperatures $T > T_g$. The curves exhibit a well developed α absorption in the low frequencies region followed by an apparently single weak absorption at high frequencies, the intensity of which increases

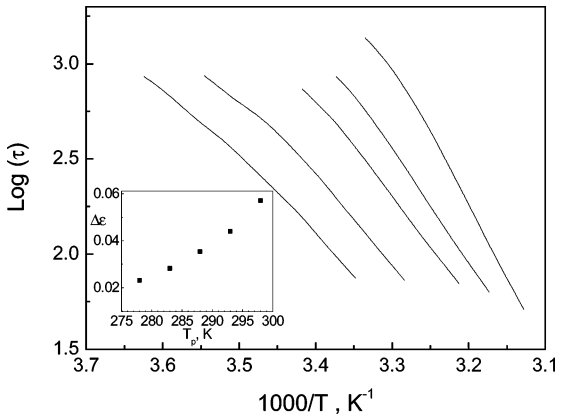

Figure 4. Arrhenius plots for the relaxation times associated with partial TSDC curves. The inset shows the variation of the dielectric strength with the poling temperature.

with temperature. As temperature increases, the α relaxation moves faster to higher frequencies than the secondary absorption as a consequence of its high activation energy. However, a temperature is reached over which the activation energy of the α relaxation and that of the secondary absorption are comparable and the distance between the two peaks remains apparently constant at moderate temperatures. This fact suggests that the fast peaks in the dielectric isotherms may not correspond their mechanism to the β relaxation observed in poly(*n*-alkyl methacrylates).

Deconvolution of Overlapping Relaxations. (A) Thermostimulated depolarization currents below T_g. A common characteristic of the ac loss curves is that the degree of overlapping of the responses of different mechanisms increases with increasing frequency. This means that the lower the frequency, the better the separation of otherwise overlapped peaks. Global TSDC peaks have an equivalent frequency given by[25]

$$f_{eq} = \frac{1}{2\pi\tau(T_m)} = \frac{hE_a}{2\pi k T_m^2} \quad (1)$$

where $h = dT/dt$ is the heating rate, k is Boltzmann's constant, E_a is the activation energy associated with the TSDC peak, τ is the relaxation time associated with the peak, and T_m is the temperature at the peak maximum. Partial depolarization curves obtained in the temperature window where the β process appears as a shoulder of the α relaxation were used to obtain ac absorptions at low frequencies. This task involves the evaluation of the relaxation time and the dielectric strength for each partial depolarization curve.

The temperature dependence of the average relaxation time associated with each TSDC peak can be written as[26]

$$\tau(T) = \frac{\int_{T_1}^{T} J(T)\, dT}{hJ(T)} \quad (2)$$

where *J(T)* is the thermal depolarization current density, and T_i is the initial depolarization temperature for each depolarization curve. The variation of the relaxation times for several partial depolarization curves with the reciprocal of temperature is given in Figure 4. It can be seen that the relaxation times of at least the half-width temperature of the peak follow Arrhenius behavior. On the other hand, the strength of each partial depolarization curve can quantitatively be expressed by[27,28]

$$\Delta\epsilon = \frac{\int_{T_0}^{T_\infty} J(T)\, dT}{\epsilon_0 hE} \quad (3)$$

where ϵ_0 is the dielectric permittivity in vacuo, E is the electric polarization field, and T_0 and T_∞ represent the extreme temperatures at the low and high-temperature sides of the peaks, respectively. The values of the dielectric strength obtained from eq 3 are given in the inset of Figure 4. The dielectric loss in the frequency domain can tentatively be obtained from eqs 2 and 3 by means of the following expression[27−29]

$$\epsilon''(\omega) = \sum_{i=1}^{n} \frac{\omega_i \tau_i(T) \Delta\epsilon_i}{1 + \omega^2 \tau_i^2(T)} \quad (4)$$

Values of the dielectric loss in the frequency domain were obtained from eq 4 in the interval of temperatures in which the β process appears as a shoulder of the α relaxation in the global TSDC curve (Figure 2). The pertinent loss isotherms corresponding to the β relaxation, given in Figure 5, are nearly symmetric peaks that shift to higher frequency with increasing temperature. Moreover, the intensity of the peaks increases as temperature goes up.

(B) Retardation Spectra above T_g. According to the linear phenomenological theory of dielectrics, the dielectric loss in the frequency domain is related to the retardation spectra by[9,11]

$$\epsilon''(\omega) = \left(\frac{\sigma}{\epsilon_0 \omega}\right)^s + \int_{-\infty}^{\infty} L(\ln \tau) \frac{\omega\tau}{1 + \omega^2\tau^2} d(\ln \tau) \quad (5)$$

where σ and ϵ_0 are the ionic conductivity and the dielectric permittivity in vacuo, respectively, while s accounts for the departure of the conductive contribution to the loss from pure ionic conductivity ($s = 1$) as a consequence of interfacial blocking electrodes effects and other phenomena. In the theory, the retardation spectrum, $L(\ln \tau)$, represents the distribution of Debye type relaxations with retardation times lying in the range between 0 and ∞. Taking into account that a Debye type relaxation is a single-exponential decay function in time domain, which becomes a Dirac δ function in the relaxation spectrum, deconvolution of overlapping peaks is better resolved in the time spectrum than in the frequency domain. It should be stressed, however, that retardation spectra, though very useful for the deconvolution of overlapping peaks, may not reflect the physical basis of relaxation processes.

The relation between the dielectric loss and the retardation spectrum is an ill-posed equation, and inversion of eq 5 to get $L(\ln \tau_k)$ is approximately accomplished from the also ill-posed quadratic programming minimization of[30]

$$\sum_{i=1}^{n} \left| \frac{\epsilon''(\omega_i)}{\rho_i} - \left(\sum_{k=1}^{m} R_{ik} L_k (\ln \tau_k) + \left(\frac{\sigma}{\epsilon_o \omega_i}\right)^s \right) \cdot \frac{1}{\rho_i} \right|^2 + \lambda [\mathbf{L}^T][\mathbf{H}][\mathbf{L}] \quad (6)$$

varying the retardation times vector ($\boldsymbol{L}$), the ionic conductivity (σ) and the exponent s. Notice that

$$R_{ik} = \frac{\omega_i \tau_k}{1 + \omega_i \tau_k^2} \ln\left(\frac{\tau_{k+1}}{\tau_{k-1}}\right)^{1/2}$$

is the term *ik* of the $n \times m$ (m > n) matrix $\boldsymbol{R}$ and $L_k(\ln \tau_k)$ is the equal log spaced retardation time vector $\mathbf{L}$ with (*m*)

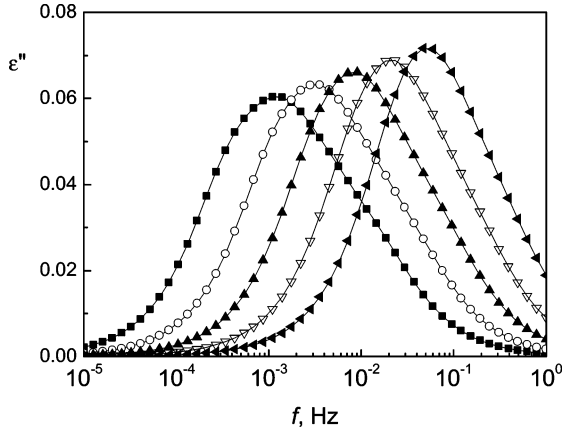

Figure 5. Frequency dependence of the simulated dielectric loss from partial TSDC data, in the range of temperature 298−318 K, 5 K step, for P24FM. The curves were obtained by means of eq 4.

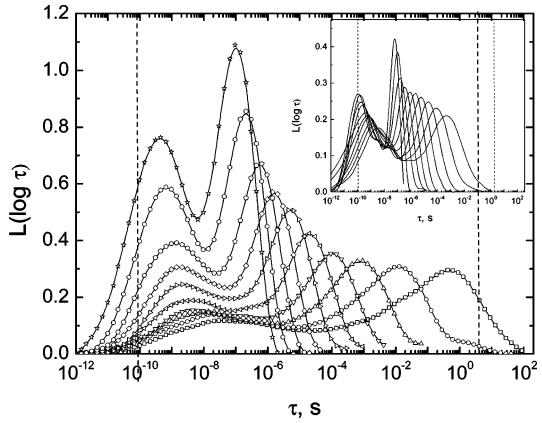

Figure 6. Retardation spectra of P24FM at several temperatures lying in the range 333−423, 10 K step. The retardation spectra of P3FM covering 333−423 K, 10 K step, are shown in the inset. The dashed lines indicate that out of the limits the values of $L(\log \tau)$ should be regarded as approximate.

elements.[19,23] The parameter $\epsilon''(\omega_i)$ in eq 6 represents the experimental value of the dielectric loss at frequency ω_i and ρ_i denotes the absolute experimental error involved in its measurement. The factor λ (>0) is a regularization parameter[31] and **H** is a definite positive quadratic form, the election of which must be based on the a priori knowledge of the solution. If the solution is thought to be piecewise linear, a good choice is $\mathbf{H} = \mathbf{B}^T\mathbf{B}$ where **B** is the $(m - 2) \times m$ matrix[30]

$$\mathbf{B} = \begin{bmatrix} -1 & 2 & -1 & 0 & 0 & \cdots & 0 \\ 0 & -1 & 2 & -1 & 0 & \cdots & 0 \\ \cdots & & & & & & \\ 0 & \cdots & & -1 & 2 & -1 & 0 \\ 0 & \cdots & & 0 & -1 & 2 & -1 \end{bmatrix} \tag{7}$$

and $\mathbf{B}^T$ is read as the transpose of the matrix **B**. The advantage of this procedure over other alternative methods commonly used to determine the retardation spectra of loss isotherms is discussed elsewhere.[19,23]

Retardation spectra of P24FM at several temperatures are shown in Figure 6. In general, the loss curves recalculated from the spectra fit pretty well to the experimental ones as the curve at 333 K, plotted as an example in Figure 7, shows. The relative experimental error is in the most unfavorable cases lower than ±3%. In general, the spectra exhibit two well developed and completely separated peaks whose intensities seem to increase with temperature though they do not merge into a single

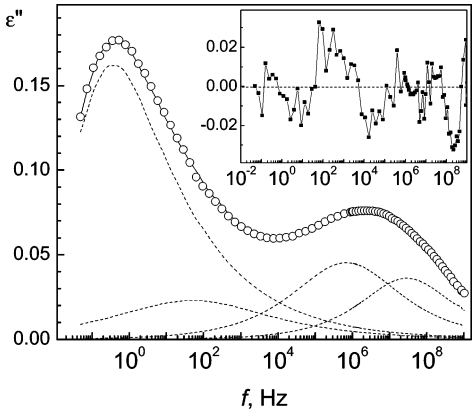

Figure 7. Reconstruction of the dielectric loss from the distribution of retardation times for P24FM, at 333 K. Open circles represent the experimental data, dashed lines the individual processes contributions while the continuous line represents the dielectric loss calculated as the sum of the individual processes. In the inset, the relative error calculated as $(\epsilon''_{REC} - \epsilon''_{EXP})/\epsilon''_{EXP}$ for all the range of frequencies.

absorption at moderate temperatures above T_g, as usually occurs in many glass formers. Since the global TSDC curves display the β process as a shoulder of the α absorption, it is important to analyze whether the longest time peak in the spectra corresponds to a genuine α relaxation. The retardation spectrum associated with the α relaxation is obtained from the inverse of the Havriliak−Negami equation yielding[10,11,32]

$$L_a(\ln \tau) = \frac{1}{\pi} \frac{(\tau/\tau_{HN})^{ab} \sin b\theta}{[(\tau/\tau_{HN})^{2a} + 2(\tau/\tau_{HN})^a \cos a\pi + 1]^{b/2}} \tag{8}$$

where the parameter θ can be written as

$$\theta = \arctan\left(\frac{\sin \pi a}{(\tau/\tau_{HN})^a + \cos \pi a}\right) \tag{9}$$

if the arguments of arc tan is positive. If it is negative, then

$$\theta = \arctan\left(\frac{\sin \pi a}{(\tau/\tau_{HN})^a + \cos \pi a}\right) + \pi \tag{10}$$

In these expressions, τ_{HN} is a characteristic retardation time, and a and b are, respectively, the shape parameters of the H−N equation that account for the departure of the α relaxation from a Debye process (the lower a, the wider the distribution of retardation times) and the skewness of the arc along a straight line toward the high-frequency region. By using $b = 1$, eq 8 also fits the spectra of secondary relaxations. The fitting of eq 8 to the longest times peak is poor unless the peak is considered a combination of the α and β relaxations, as the global and partial TSDC curves suggest. The deconvoluted retardation times peaks for α and β processes, shown at different temperatures in Figure 8, become narrower with increasing temperature. On the other hand, successful fitting of eq 8 to the shortest times absorption of the spectra requires to assume it as the result of the overlapping of two processes named γ and γ', respectively in increasing order of time. The temperature dependence of the shape parameters that define the α, β, γ', and γ relaxations are given at different temperatures in Figure 9. In general, the shape parameters tend to increase with increasing temperature.

The dielectric strength for different processes can be obtained from the spectra by means of the following expression

$$\epsilon_{r;i} - \epsilon_{u;i} = \int_{-\infty}^{\infty} L_i(\ln \tau)\, d(\ln \tau) \tag{11}$$

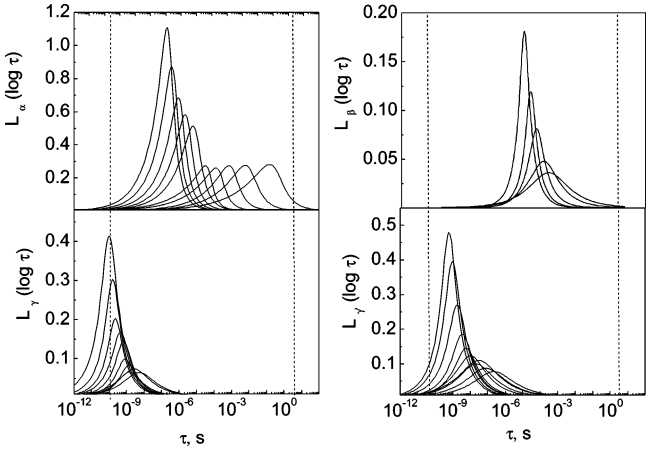

Figure 8. Retardation spectra from 323 to 423 K corresponding to the α (top left), γ (bottom left), β (top right), and γ' (bottom right) relaxations, at 10 K step, for P24FM. The dashed lines indicate that out of the limits the values of $L(\log \tau)$ should be regarded as approximate.

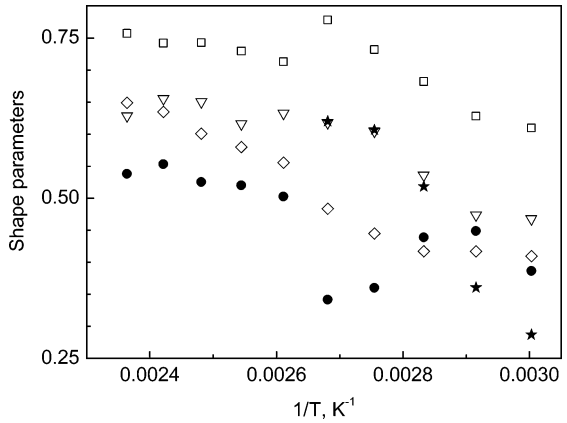

Figure 9. Temperature dependence of the fitting parameters of the HN equation for the α, β, and γ relaxations of P24FM. Square and circles refer to the *a* and *b* parameters of the HN equation; stars, triangles, and rhombus represent the *a* parameter of the HN equation, with $b = 1$, for the β, γ', and γ relaxation processes, respectively.

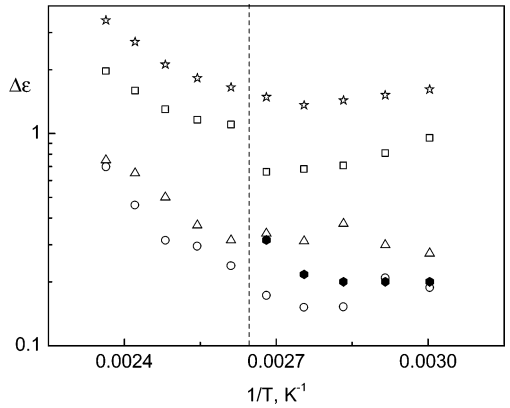

Figure 10. Variation of the dielectric strengths of the α (squares), β (filled hexagon), γ (triangles), γ' (circles) relaxations, and total relaxation strength (stars) with the reciprocal of temperature for P24FM. The dashed line indicates the merging temperature of α and β relaxations forming the αβ absorption.

where the subscript *i* refers to the type of relaxation (α, β, γ', γ). The temperature dependence of the dielectric strengths is shown in Figure 10. It can be seen that the strength of the α absorption slightly decreases with increasing temperature until a temperature is reached above which this process undergoes a rather sharp increase as temperature goes up. This increase is also observed in the dielectric strengths of the secondary relaxations.

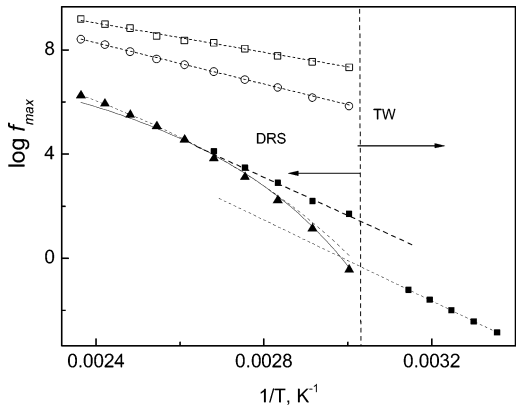

Figure 11. Arrhenius plots for the peak maxima of the relaxation processes. Open squares and circles refer to the secondary γ and γ' relaxations, respectively, while filled squares and triangles represent the temperature dependence of the β and α absorptions, respectively. The data below T_g corresponding to the β relaxation were obtained from partial TSDC curves.

Temperature Dependence of the Relaxation Processes. Figure 11 shows the temperature dependence of the frequency associated with the peak maxima ($f_{max} = {}^1/_{2\pi\tau_{max}}$) of the α, β, γ', and γ relaxation processes. The secondary absorptions follow Arrhenius behavior with activation energies of 55 ± 2, 76.8 ± 0.8, and 144 ± 6 kJ/mol, respectively, for the γ, γ', and β relaxations. The activation energy associated with the β absorption obtained from partial thermostimulated depolarization current curves is 148.7 ± 0.2 kJ/mol, near to that obtained from dielectric relaxation spectroscopy. As usual, the curve log f_{max} vs $1/T$ for the α absorption is described by the VFTH equation[7]

$$f_{max} = f_0 \exp\left(-\frac{m}{T - T_V}\right) \tag{12}$$

where f_0 is a prefactor of the order of the reciprocal of picoseconds, m is a constant and T_V is the Vogel temperature. The values of m and T_V that fit the VFTH equation to the experimental results are, respectively, 1800 ± 300 K and 266 ±7 K. Departure of the α process from Arrhenius behavior is defined by the fragility factor $D = m/T_V$ that controls how closely a system obeys the Arrhenius law.[33] The fragility factor for P24FM is 6.8, a value below the borderline that separates fragile ($D < 10$) from strong ($D > 10$) glasses.

The ionic conductance follows Arrhenius behavior as the plot of Figure 12 shows. The value of the activation energies obtained from the slope of the plot amounts to 177 ± 2 kJ/mol. Therefore, ionic transport in P24FM overcomes energy barriers of the order of those involved in the β process. In the inset, the variation with temperature of the exponent *s* that accounts for the departure of the ionic contribution to the loss from pure conductivity is also shown. The results suggest that interfacial blocking electrodes effects and other phenomena become less and less important with increasing temperature.

Discussion

An excess contribution or "excess wing" to the high-frequency peak of the α relaxation is observed in broadband dielectric spectra of supercooled liquids.[34−36] Theoretical explanations for its occurrence have been proposed[37,38] though no consensus on the microscopic origin of this phenomenon has been reached.[39] On the other hand, the spectra of many glass-

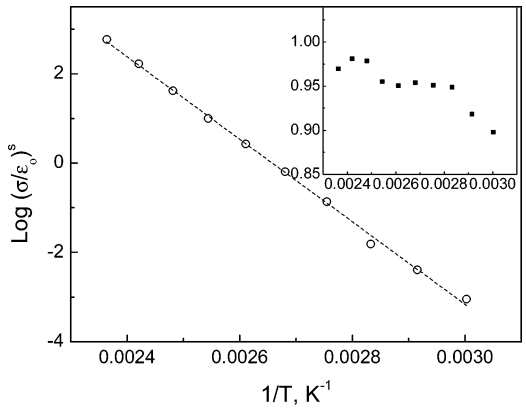

Figure 12. Arrhenius plot for the conductivity contribution of P24FM to the dielectric loss. The conductivity is given in S/m. The inset shows the variation of the exponent s in eq 5 with temperature.

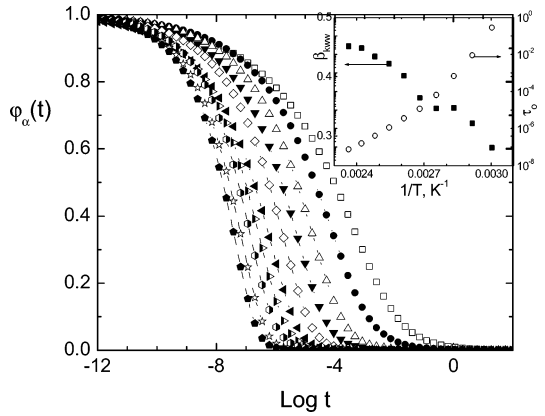

Figure 13. Normalized relaxation curves in the time domain for the α relaxation of P24FM, in the range of temperature 333−423 K at 10 K steps. The decay curves (circles) are fitted (dashed line) by the KWW equation using the stretch exponents β_{KWW} and the characteristic relaxation times τ_0 shown in the inset of the figure.

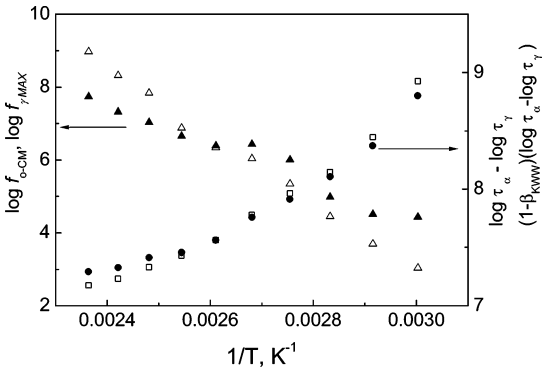

Figure 14. Fitting of Ngai's criteria to experimental results for the γ relaxation. See text for details.

forming materials display a well-developed β relaxation. Although intramolecular motions were held responsible for β relaxations, Johari and Goldstein[40] demonstrated that the relaxation also shows up in rigid molecules where intramolecular conformational transitions are unlikely. This fact led to postulate that the so-called Johari−Godstein (JG) β relaxation is inherent to glass forming materials in general.[40,41] Although until recently it was thought that the excess wing and the JG β relaxations are due to different processes,[42,43] some strong experimental hints have emerged that the excess wing is merely the high frequency of a β peak, hidden under the dominating α peak.[44] Recently, it has been reported that the excess wing rather than higher frequency relaxations adscribed to the JG β process is perhaps a universal feature of glass formers, albeit not always discernible at ambient pressure.[45] In principle, the slowest secondary relaxation of P24FM reminds an excess wing contribution to the α relaxation, but its deconvolution from longest time peak of the retardation spectra together with the merging of this secondary relaxation with the α absorption at a temperature not far above from T_g also suggests that it could be a β process.

Many authors considered the JG β relaxation as a precursor of the α and have tried to relate them. Guided by the coupling model, Ngai[46,47] found that the JG β relaxation obeys two criteria: (1) $\tau_\beta(T_g\alpha) \approx \tau_0(T_g\alpha)$ where $\tau_0 = t_c^n \tau_\alpha^{1-n}$ and (2)

$$\log(\tau_\alpha) - \log(\tau_\beta) \approx n(\log \tau_\alpha - \log t_c) \qquad (13)$$

In these two expressions, $n = 1 - \beta_{KWW}$ is the coupling parameter, t_c is a temperature insensitive crossover time and β_{KWW} is the stretch exponent of the KWW equation. With the aim of investigating whether the β relaxation detected in P24FM obeys to these results, the normalized decay function describing the α process in the time domain was calculated at different temperatures from the retardation spectra by means of the following expression

$$\varphi_\alpha(t) = \frac{\int_{-\infty}^{\infty} L_\alpha(\ln \tau) e^{-t/\tau} \, d(\ln \tau)}{\int_{-\infty}^{\infty} L_\alpha(\ln \tau) \, d(\ln \tau)} \qquad (14)$$

Curves representing the decay function for the α relaxation are plotted at several temperatures in Figure 13. As usual, the α relaxation in the time domain is inevitably described by a stretch exponential or decay function such as[1]

$$\varphi_\alpha(t) = \exp[-(t/\tau_0)^{\beta_{KWW}}] \qquad (15)$$

where the stretch exponent lies in the range $0 < \beta_{KWW} \leq 1$. The values of β_{KWW} and τ_0 that fit eq 15 to the decay functions are plotted in the inset of Figure 13. It can be seen that the stretch exponent increases with increasing temperature.

The slowest relaxation of P24FM does not obey to the Ngai criteria for a JG process since $\tau_\beta(T_g\alpha)| \gg \tau_0(T_g\alpha)$ in the whole temperature range. The second criterion $\tau_\alpha/\tau_\beta \approx (\tau_\alpha/t_c)^{1-\beta_{KWW}}$ neither holds. These criteria, however, hold pretty well in a wide range of temperature for the fastest relaxation (γ process) as the plots of Figure 14 show. However, the secondary absorption γ' only roughly obeys the two criteria.

The coupling model suggests that the activation energy of the β process is related to the glass transition temperature by the expression[48]

$$\frac{E_a}{RT_g} = 2.303(2 - 13.7n - \log \tau_\infty) \qquad (16)$$

where $n = 1 - \beta_{KWW}$. The results of E_a/RT_g calculated from eq 16 for the β relaxation is 41.6 in fair agreement with the experimental result, 48.4. However, it is instructive to point out that eq 16 yields 27.6 and 22.4 for the γ' and γ processes, in rather good agreement the experimental ones which amount to 25.9 and 18.5, respectively.

Although intermolecular interactions surely contribute to the response of the condensed matter to the perturbation fields, intramolecular interactions in polymers presumably play a leading role in the development of secondary absorptions. In this regard, it is tempting to compare the spectra of P24FM and P3FM since the direction of the dipole associated with the

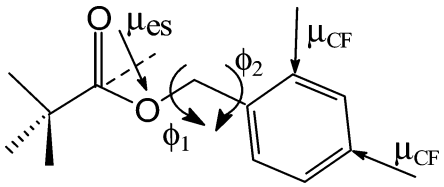

Figure 15. Sketch of the side chain of P24FM showing the rotational angles and the directions of the dipole moments associated with the ester group, μ_E, and the C−F bonds, μ_{CF}.

phenyl group of P3FM coincides with that of the dipole resulting from the vectorial sum of the two C^{ar}−F dipoles of P24FM. Retardation spectra of P3FM at different temperatures are shown in the inset of Figure 6. Though two peaks appear in the spectra of both polymers, their overlapping at high temperature is larger for P24FM than for P3FM. On the other hand, the curves describing the temperature dependence of the global thermal stimulated depolarization current present in both cases the β process as a shoulder of the α relaxation. Moreover, the γ absorption is significantly wider for P24FM than for P3FM.

Let us consider now the molecular motions responsible for the development of the subglass relaxations in P24FM. A rough sketch of the isolated side group chain is given in Figure 15 where the rotational angles over CO−CH_2C^{ar} (ϕ_1), $COCH_2$−C^{ar} (ϕ_2) and the dipoles associated with the ester group (μ_{es} = 1.89 D)[49] and the C^{ar}−F bonds (μ_{CF} = 1.45 D)[50] are shown. As is well-known, *C*(*O*)−O bonds in ester moieties are restricted to trans states.[51,52] As described elsewhere,[53] 36^2 conformations were generated by rotations about the ϕ_1 and ϕ_2 bonds and the energy of each conformation was minimized with respect to all other internal coordinates. The probability of each conformation was calculated as

$$p(\phi_1,\phi_2) = \frac{1}{2}\left(-\frac{E(\phi_1,\phi_2)}{RT}\right) \qquad (17)$$

where *Z* is the partition function. The curves of probability show that staggered orientations (i.e., $\phi_1 = 0, \pm 60$) are preferred by the CO−CH_2C^{ar} rotation while $\phi_2 = 0, \pm 40$; $180, \pm 40$ are favored by the $COCH_2$−C^{ar} bond. Rotations of different sign (i.e., $\phi_1 = 60$, $\phi_2 = 40$) give rise to strong repulsive interactions among the oxygen atom of the carbonyl group and the H or F atoms attached to the phenyl group, and therefore are forbidden. By extending the conformational analysis of isolated side chains to polymers we realize that the nonplanar conformations preferred in the former case would produce severe repulsions among neighboring units.[53] Moreover, among the four planar conformations (ϕ_1, $\phi_2 = 0, 180°$), that one ($\phi_1 = 0$) giving rise to cis conformations over the CO−CH_2C^{ar} bond are of high energy due to strong repulsive interactions within the group and therefore are forbidden. This analysis leads to conclude that the conformations preferred by the side chains are of planar type, specifically, $\phi_1 = 180$, $\phi_2 = 0$ and $\phi_1 = 180$, $\phi_2 = 180$. The dipole moments and the energies of these conformations are, respectively, 0.31 D and 5.21 kJ/mol for the first conformation, and 2.74 D and 3.1 kJ/mol for the latter. Fluctuations of the phenyl groups in these minima may be responsible for the γ and γ' relaxations in the spectra. In the case of P3FM,[24] the location of the fluorine atom in the position 3 of the phenyl group produces lower interactions than in the case of the fluorine atom located in position 2 in P24FM. The nearly freely rotating CH_2−C^{ar} bonds of P3FM give rise to the simple γ absorption observed in the spectra of this polymer. It is worth noting that only the γ relaxation in the spectra of P24FM, the absorption of lowest activation energy (E_a = 55 kJ/mol), meets the two requirements stated by Ngai for a JG β absorption. However, since the absorption arises from motions of the bulky difluorinated phenyl group and not from motions of the whole side chain coupled with motions of a very few skeletal bonds of the main chain, the relaxation is not a JG β process.

The β relaxation is extremely sensitive to the chemical structure. The molecular mechanism behind the β relaxation of poly(methyl methacrylate) is postulated to be hindered rotation of the ester moiety about the C−C(O) bond that connects it to the main chain, though involving some sort of intramolecular cooperativity.[14] The polarization arising from the electric dipole associated with carboxyl group relaxes through the β relaxation and only a smaller part through the main chain dynamics reflected in the α relaxation. As a result this polymer exhibits a very strong β process and a rather weak α relaxation. For poly(*n*-alkyl methacrylate)s with $n > 1$, the polarization relaxes through the β relaxation and also a significant part through segmental motions associated with the α relaxation.[20,22] Similar behavior is observed for other polymers.[1,19] The β relaxation of P24FM presumably arises from generalized motions about the skeletal bonds of the side groups combined with motions of a very few skeletal bonds of the main chain. These complex motions superpose with the segmental motions of the α relaxation in such a way that the β process becomes hidden by the α absorption. This behavior is also observed in the chain dynamics of P3FM and other poly(benzyl methacrylates) with a hydrogen of the phenyl groups substituted by a methyl group or a chlorine atom.[24] It is noticeable that the intensity of the β peak in phenyl-substituted poly(benzyl methacrylate)s is lower than in the case of poly(*n*-alkyl methacrylate)s, probably as a consequence of the bulkiness of the lateral chain in the former case.

The relaxation behavior P24DFM can qualitatively be explained in terms of the energy landscape of amorphous chains. In Stillinger's view,[54] the conformational energy landscape of supercooled liquids is formed by craters connected by small basins. The small basins also are present inside the craters. The lower the temperature, the rarer and more separated the craters must be. Secondary processes are identified with elementary relaxations between neighboring basins while α relaxations entail escape from a deep basin or crater and eventually into another. Escape from a crater to another one requires a lengthy direct sequence of elementary transitions. The activation energy associated with the β absorption of P24FM is rather large, of the order of 144 k J/mol, suggesting the presence of big basins or minicraters in the topology of the energy landscape, in addition to the craters. Then the β absorption would be the result of minicrater structural relaxation through small basins. As temperature decreases, the density of craters in the energy landscape becomes rarer until conformational transitions between them are not longer possible and the system turns a glass. However, minicraters and basins remain operative below the glass transition temperature. At high temperature, β and α relaxations exhibit the same temperature dependence, a scenario not commonly found in the relaxation behavior of supercooled liquids. This behavior indicates a strong interdependence between α and β processes in this region presumably as a result of the similarity of the energy landscape of both processes.

The total dielectric strength of P24FM is significantly higher than that of P3FM as a consequence of the following facts: there are energetically favorable conformations in the former polymer arising from rotations about CH_2−C^{ar} bonds in which the C^{ar}−F dipole located in position 2 becomes favorably oriented to the carbonyl group. On the other hand, the orientation of the C^{ar}−F dipole of P24FM in position 4 lies in the direction of the

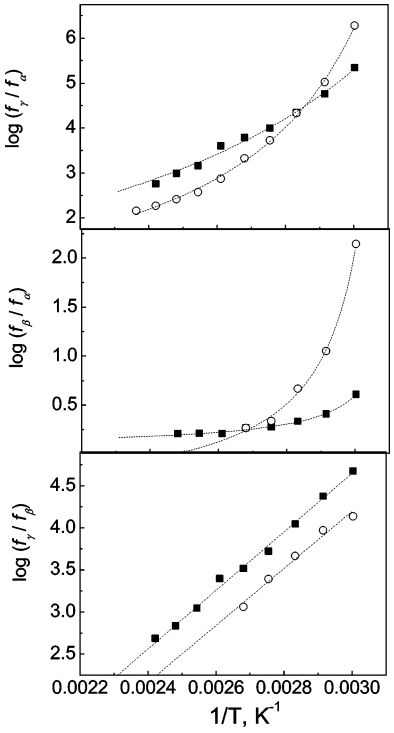

Figure 16. Variation of the distance between the maxima of the γ and β peaks with temperature for P24FM (open symbols) and P3FM (filled symbols).

CH_2-C^{ar} bond and therefore its orientation with respect to the direction of the dipole of the ester groups does not depend on ϕ_2. However, as a result of ϕ_1 rotation, the dipole located in position 4 in the phenyl group contributes to the dielectric strength of the polymer.

The distance between the maxima of the deconvoluted α and β peaks, expressed in terms of $\Delta_{\beta-\alpha} = \log (f_{\max,\beta}/f_{\max,\alpha})$, is plotted as a function of temperature for P24FM and P3FM[23] in Figure 16. As usual, $\Delta_{\beta-\alpha}$ decreases with increasing temperature until the distance eventually vanishes. The temperatures at which this occurs are 378 and 383 K for P24FM and P3FM, respectively. The temperature dependence of Δ_β-α is described by a Vogel type equation, the values of T_V being 271 and 319 K, respectively, for P3FM and P24FM. Notice that these values of T_V are close to the respective glass transition temperatures. Similar behavior is found for $\Delta_{\gamma-\alpha} = \log (f_{\max,\gamma}/f_{\max,\alpha})$, but in this case the values of T_V are below T_g, specifically, 292 and 216 K for P24FM and P3FM, respectively. Finally the temperature dependence of the distance between the secondary peaks, for example, $\Delta_{\gamma-\beta} = \log (f_{\max,\gamma}/f_{\max,\beta})$, is a linear function of the reciprocal of the absolute temperature as a consequence of the fact that secondary processes follow Arrhenius behavior.

Conclusions

Polymers with flexible polar side groups exhibit high conformational versatility which strongly affects the response of these substances to external force fields. The spectra of these materials are characterized for displaying a long time peak well separated from a short time peak. Extrapolation methods predict that the merging of the two peaks occurs at unrealistic high temperatures. The long times peak is characterized for hiding the β relaxation, and both the α and β relaxations exhibit the same temperature dependence not far above the glass transition temperature. This scenario suggests that the energy landscape in this range of temperatures is rather similar for both processes. Differences in the response of polymers to force fields are shifted to shorter times as the differences in their fine structures decrease.

Acknowledgment. This research was supported by the DGICYT through Grants MAT2005-05648-C02-01/-02.

References and Notes

(1) Williams, G. *Adv. Polym. Sci.* **1979**, *39*, 59.
(2) Williams, G. In *Keynote Lectures in Selected Topics of Polymer Science*; Riande, E.; Ed.; CSIC: Madrid, 1995; Chapter 1.
(3) Doi, M.; Edwards, S. F. *The Theory of Polymer Dynamics*; Clarendon Press: Oxford, U.K., 1986.
(4) de Gennes, P. G. *Scaling Concepts in Polymer Physics*, 2nd ed.; Cornell University Press: Ithaca, NY, 1985.
(5) Stockmayer, W. H. *Pure Appl. Chem.* **1967**, *15*, 539. Adachi, K.; Kotaka, T. *Macromolcules* **1984**, *17*, 120.
(6) Ferry, J. D. *Viscoelastic Properties of Polymers*; Wiley: New York, 1970.
(7) Vogel, H. *Z. Phys.* **1923**, *22*, 645. Fulcher, J. S. *J. Am. Ceram. Soc.* **1925**, *8*, 839. Tammann, G.; Hesse, W. *Z. Anorg. Allg. Chem.* **1926**, *156*, 245.
(8) Williams, G. *Trans. Faraday Soc.* **1964**, *62*, 2091.
(9) McCrum, N. G.; Read, B. E.; Williams, G. *Anelastic and Dielectric Effects in Polymeric Solids*; Wiley: New York, 1967; Chapter 4.
(10) Schönhals, A. In *Broadban Dielectric Spectroscopy*; Springer-Verlag: Berlin 2003; Chapter 7.
(11) Riande, E.; Díaz-Calleja, R. *Electrical Poperties of Polymers*, Marcel Dekker: New York, 2004; Chapter 8.
(12) Bergman, R.; Alvarez, F.; Alegría, A.; Colmenero, J. *J. Chem. Phys.* **1998**, *109*, 7546.
(13) McCrum, N. G.; Read, B. E.; Williams, G. *Anelastic and Dielectric Effects in Polymeric Solids*; Wiley: London, 1967; Chapter 8.
(14) S. C. Kuebler, D. J. Schaefer, C. Boeffel, U. Pawelzik, H. W. Spiess *Macromolecules* **1997**, *30*, 6597. Gómez, D.; Alegría, A.; Arbe, A.; Colmenero, J. *Macromolecules* **2001**, *34*, 503.
(15) Schröter, K.; Unger, R.; Reissig, S.; Garwe, F.; Kahle, S.; Beiner, M.; Donth, E. *Macromolecules* **1998**, *31*, 8966.
(16) Kahle, S.; Korus, J.; Hempel, R.; Unger, R.; Höring, S.; Schröter, K.; Donth, E. *Macromolecules* **1997**, *30*, 7214.
(17) Casalini, R.; Fioretto, D.; Livi, A.; Luchéis, M.; Rolla, P. A. *Phys. Rev. B* **1997**, *56*, 3016.
(18) Huang, Y.-N.; Saiz, E.; Ezquerra, T.; Guzmán, J.; Riande, E. *Macromolecules* **2002**, *35*, 2926.
(19) Álvarez, C.; Lorenzo, V.; Riande, E. *J. Chem. Phys.* **2005**, *122*, 194905.
(20) Garwe, F.; Schönhals, A.; Lockwenz, H.; Beiner, M.; Schröter, K.; Donth, E. *Macromolecules* **1996**, *29*, 247.
(21) Schröter, K.; Unger, R.; Reissig, S.; Garwe, F.; Kahle, S.; Beiner, M.; Donth, E. *Macromolecules* **1998**, *31*, 8966.
(22) Kahle, S.; Korus, J.; Hempel, R.; Unger, R.; Höring, S.; Schröter, K.; Donth, E. *Macromolecules* **1997**, *30*, 7214.
(23) Dominguez-Espinosa, G.; Díaz-Calleja, R.; Riande, E.; Gargallo, L.; Radic, D. *J. Chem. Phys.* **2005**, *123*, 114904.
(24) Dominguez-Espinosa, G.; Díaz-Calleja, R.; Riande, E.; Gargallo, L.; Radic, D. *Macromolecules* **2006**, *39*, 3071.
(25) van Turnhout, J. *Thermally Stimlated Discharge of Polymer Electretes*; Elsevier, Ámsterdam, 1975.
(26) Bucci, C.; Fieschi, R.; Guidi, G. *Phys. Rev.* **1966**, *148*, 816.
(27) Shimizu, H.; Nakayama, K. *J. Appl. Phys.* **1993**, *74*, 1597.
(28) Díaz-Calleja, R.; Sancís, M. J.; Alvarez, C.; Riande, E. *J. Appl. Phys.* **1997**, *81*, 3685.
(29) Perlman, M. M.; Unger, S. *J. Appl. Phys.* **1974**, *45*, 2389.
(30) Press, W. H.; Teukolsky, S. A.; Vetterling, W. T.; Flannerty, B. P. In *The Art of Scientific Computing*, 2nd ed.; Cambridge University Press: New York, 1992; Chapter 18.
(31) Morozov, V. A *Methods for Solving Incorrectly Posed Problems*; Springer: New York, 1984.
(32) Reiner Zorn, A. *J. Polym. Sci., Part B: Polym. Phys.* **1999**, *37*, 1043.
(33) Angell, C. A. In *Complex Behavior of Glassy Systems*, Proceedings of the XIV Sitges Conference, Sitges, Barcelona, Spain, 10−14 June 1996; Rubí, M., Pérez-Vicente, C., Eds., Springer-Verlag: Berlin, 1997.
(34) Hofmann, A.; Kremer, F.; Fisher, E. W.; Schönhals, A. In *Disorder Effects on Relaxational Processes*; Richert, R., Blumen, A., Eds.; Springer: Berlin, 1994; p 309.
(35) Dixon, P. K.; Wu, L.; Nagel, S. R.; Williams, B. D.; Carini, J. P. *Phys. Rev. Lett.* **1990**, *65*, 1108.
(36) Kudlik, A.; Benkhof, S.; Blochowicz, T.; Tschirwitz, C.; Rössler, E. *J. Mol. Struct.* **1999**, *479*, 201.

(37) Chamberlein, R. V. *Phys. Rev. B* **1993**, *48*, 15638.
(38) Chamberlein, R. V. *Phys. Rev. Lett.* **1999**, *82*, 2520.
(39) Lukenheimer, P.; Loidl, A. *Chem. Phys.* **2002**, *284*, 205.
(40) Johari, G. P.; Goldstein, M. *J. Chem. Phys.* **1970**, *53*, 2372.
(41) Johari, G. P. *Ann. N.Y. Acad. Sci.* **1976**, *279*, 117.
(42) Dixon, P. K.; Wu, L.; Nagel, S. R.; Williams, B. D.; Carini, J. P. *Phys. Rev. Lett.* **1990**, *65*, 1108.
(43) Kudlik, A.; Benkhof, S.; Blochowicz, T.; Tschirwitz, C.; Rössler, E. *J. Mol. Struct.* **1999**, *479*, 201.
(44) Schneider, U.; Brand, R.; Lunkenheimer, P.; Lidl, A. *Phys. Rev. Lett.* **2000**, *84*, 5560.
(45) Casalini, A.; Roland, C. M. *Phys. Rev. Lett.* **2003**, *91*, 15702.
(46) Ngai, K. L. *J. Chem. Phys.* **1998**, *109*, 6982.
(47) Ngai, K. L.; Paluch, M. *J. Chem. Phys.* **2004**, *120*, 857.
(48) Ngai, K. L. Capacioli, S. *Phys. Rev. E* **2004**, *69*, 031501.
(49) Saiz, E.; Hummel, J. P.; Flory, P. J.; Plavsic, M. *J. Phys. Chem.* **1981**, *85*, 3211.
(50) McClellan, A. L. *Tables of Experimental Dipole Moments*, Rahara Enterprises: El Cerrito, CA, 1974; Vol. II. *Tables of Experimental Dipole Moments*; Rahara Enterprises: El Cerrito, CA, 1989; Vol. III.
(51) Flory, P. J. *Statistical Mechanics of Chain Molecules*; Wiley-Interscience: New York, 1969.
(52) Riande, E.; Saiz, E. *Dipole Moments and Birefringence of Polymers*; Prentice Hall: Englewood Cliffs, NJ, 1992.
(53) Díaz-Calleja, R.; Sanchís, M. J.; Saiz, E.; Martínez-Piña, F.; Miranda, R.; Gargallo, L.; Radic, D. Riande, E. *J. Polym. Sci., Part B: Polym. Phys.* **2000**, *38*, 2179.
(54) Stillinger, F. K. *Science* **1995**, *267*, 1935.

MA060699E